

Rotating analogue black holes: Quasinormal modes and tails, superresonance, and sonic bombs and plants in the draining bathtub acoustic hole

José P. S. Lemos

*Centro Multidisciplinar de Astrofísica - CENTRA, Departamento de Física,
Instituto Superior Técnico - IST, Universidade de Lisboa - UL,
Av. Rovisco Pais 1, 1049-001 Lisboa, Portugal*

In *Analogue spacetimes: The first thirty years*, eds. L. C. Crispino et al (Editora Livraria da Física, São Paulo 2013), p. 145; Proceedings of the II Amazonian Symposium on Physics “Analogue Models of Gravity: 30 Years Celebration of the publication of Bill Unruh’s paper “Experimental Black-Hole Evaporation?””.

Based on the invited lecture at the Symposium realized in the Universidade Federal do Pará, Belém do Pará, Brazil, June 1 - 3, 2011.

Rotating analogue black holes: Quasinormal modes and tails, superresonance, and sonic bombs and plants in the draining bathtub acoustic hole

José P. S. Lemos¹

*Centro Multidisciplinar de Astrofísica - CENTRA, Departamento de Física,
Instituto Superior Técnico - IST, Universidade de Lisboa - UL, Av. Rovisco
País 1, 1049-001 Lisboa, Portugal*

Abstract: The analogy between sound wave propagation and light waves led to the study of acoustic holes, the acoustic analogues of black holes. Many black hole features have their counterparts in acoustic holes. The Kerr metric, the rotating metric for black holes in general relativity, has as analogue the draining bathtub metric, a metric for a rotating acoustic hole. Here we report on the progress that has been made in the understanding of features, such as quasinormal modes and tails, superresonance, and instabilities when the hole is surrounded by a reflected mirror, in the draining bathtub metric. Given then the right settings one can build up from these instabilities an apparatus that stores energy in the form of amplified sound waves. This can be put to wicked purposes as in a bomb, or to good profit as in a sonic plant.

¹joselemos@ist.utl.pt

1. Introduction

1.1 Black holes

Black holes, the most fascinating prediction of general relativity, are the simplest objects which can be built out of spacetime itself [1]. They are hard to detect. Astrophysical black holes are very far away and electromagnetically can only be inferred indirectly. The manufacturing of TeV scale black holes is a dream (see for a review [2]), whereas Planckian scale black holes are far beyond current and future energetic technological capabilities [3].

Understanding classical physical phenomena that occurs with black holes is important. For instance, black hole quasinormal modes (QNMs), which appear when a black hole is naturally perturbed, can test black hole stability and should provide means to identifying black hole parameters like the mass M , the angular momentum J , and the charge Q , from the real ω_R and imaginary ω_I parts of the mode frequencies [4–13]. Power-law tails that rise at the end of the perturbation also give insight into the black hole features and parameters [14]. Moreover, the Penrose process [15], superradiance [16–20], and black hole instabilities, such as the black hole bomb instability [21, 22], as well as no-hair theorems and their possible tests [23, 24], are phenomena that help in the making of the whole picture of what a black hole is.

Understanding of quantum phenomena is also important. Hawking showed that when quantum effects are taken into account, black holes emit thermal radiation [25]. This led to a number of fundamental questions, such as the information puzzle, black hole entropy (which in turn, following a conjecture put forward in [26], could be related to quasinormal modes with a large imaginary part and give direct information on the degrees of freedom of the quantum area cells of the black hole horizon, see also [9–13]), and the black hole final state (for a review see [27]).

1.2 Acoustic holes

There is the question posed by many physics students of why the velocity of sound is different from the velocity of light. There are many differences, of course, but in a way Unruh [28] brought them a bit closer to each other. Indeed, prospects for having a black hole in the hand changed when in 1981 Unruh [28] realized that for a fluid moving with a space-dependent velocity which exceeds the sound velocity of the medium one gets the equivalent of an event horizon for sound waves. The concept of a dumb hole or acoustic hole, the acoustic analogue of a black hole, was created. This concept has been further developed, see e.g., [29–31], and [32] for a review, where, among other things, similarities and differences between the rotating draining bathtub acoustic hole and the Kerr black hole are displayed. Many other different kinds of analogue holes have been devised involving not only fluids, but

also condensed matter systems, slow light devices, and other models [33–35]. Within these models, phonon radiation, the sonic analogue of Hawking radiation and one of the most important effects in these physical systems, has been studied with some care [36–39].

There are certainly other phenomena that occurs with true black holes that also occurs with acoustic holes. For instance, there is analogous geodesic and causal structure, and Carter-Penrose diagrams can be drawn [40]. Quasi-normal modes and power-law tails are also expected in acoustic models [41, 42], see also [43, 44]. As well, in analogy with general relativistic effects in black holes, we also expect in acoustic holes the phenomenon of superresonance [45, 46] (see also [30]), which in some cases can be amplified into a sonic bomb [41], or depending on the use into a sonic plant.

1.3 Acoustic holes in this presentation

We use the rotating draining bathtub acoustic hole [29–31], which is an analogue of the Kerr black hole. We study the QNMs of this rotating draining bathtub acoustic hole [41, 42], see also [43, 44], and the power-law tails that appear long after the initial perturbation [41]. Then, we compute the reflection coefficients for superresonant scattering in this acoustic hole background [41, 42]. Enclosing the acoustic hole by a reflecting mirror we install an instability into the system thereby turning it into a sonic bomb [41] or a sonic power plant. The worked reported in this review has been done in collaboration with Emanuele Berti, Vitor Cardoso, and Shijun Yoshida [41, 42].

2. The draining bathtub acoustic hole: the geometry

The draining bathtub model first introduced by Visser [29] for a rotating acoustic hole is the starting point (see also [30, 31]). The fluid moves in a plane, it is a 2-dimensional flow, which can be made 3-dimensional by the addition of another trivial dimension perpendicular to the original plane.

Consider a fluid having (background) density ρ . Assume the fluid to be locally irrotational (vorticity free), barotropic and inviscid. Use polar coordinates (r, ϕ) . From the equation of continuity, the radial component of the fluid velocity satisfies $\rho v^r \sim 1/r$. Irrotationality implies that the tangential component of the velocity satisfies $v^\phi \sim 1/r$. By conservation of angular momentum we have $\rho v^\phi \sim 1/r$, so that the background density of the fluid ρ is constant. In turn, this means that the background pressure p and the speed of sound c are constants. Thus one can put

$$\vec{v} = \frac{-A \hat{e}_r + B \hat{e}_\phi}{r}, \quad (1)$$

where A and B are constants and \hat{e}_r and \hat{e}_ϕ are the unit vectors in the radial and azimuthal directions, respectively. This flow velocity can be obtained as the gradient of a velocity potential, $\vec{v} = \nabla \bar{\psi}$, where

$$\bar{\psi} = A \log r + B \phi. \quad (2)$$

Perturb the fluid, and encode the perturbation in the velocity potential, so that the new velocity potential is $\bar{\psi} + \psi$, ψ being the perturbation. Unruh [28] first realized that the propagation of a sound wave in a barotropic inviscid fluid with irrotational flow is described by the following equation for ψ ,

$$\nabla_\mu \nabla^\mu \psi = 0, \quad (3)$$

where the operator ∇_μ denotes covariant derivative, and μ runs from 0 to 2, with 0 denoting a time coordinate and 1,2 spatial coordinates. This is the Klein-Gordon equation for a massless field, in this case the perturbed velocity potential ψ , in a Lorentzian acoustic curved geometry.

In our case, the acoustic metric describing the propagation of sound waves in this draining bathtub fluid flow is $(2+1)$ -dimensional and given by [29],

$$ds^2 = - \left(c^2 - \frac{A^2 + B^2}{r^2} \right) dt^2 + \frac{2A}{r} dr dt - 2B d\phi dt + dr^2 + r^2 d\phi^2, \quad (4)$$

where t is the time coordinate. In the non-rotating limit $B = 0$ the metric (4) reduces to a standard Painlevé-Gullstrand-Lemaître type metric. If one adds a dz^2 term the metric turns into a $(3+1)$ -dimensional metric. The acoustic horizon is located at

$$r_H = \frac{A}{c}. \quad (5)$$

The ergosphere forms at

$$r_{es} = \frac{(A^2 + B^2)^{1/2}}{c}, \quad (6)$$

and the angular velocity of the horizon is

$$\Omega = \frac{B}{r_H^2}. \quad (7)$$

It is useful sometimes to see the metric in a Boyer-Lindquist Kerr metric form. Transforming then to Boyer-Lindquist coordinates $(\tilde{t}, r, \tilde{\phi})$, one finds

$$ds^2 = - \left(1 - \frac{A^2 + B^2}{c^2 r^2} \right) c^2 d\tilde{t}^2 + \left(1 - \frac{A^2}{c^2 r^2} \right)^{-1} dr^2 - 2B d\tilde{\phi} d\tilde{t} + r^2 d\tilde{\phi}^2. \quad (8)$$

The geodesics of a test particle in Boyer-Lindquist coordinates can be seen in Fig. 1 [44].

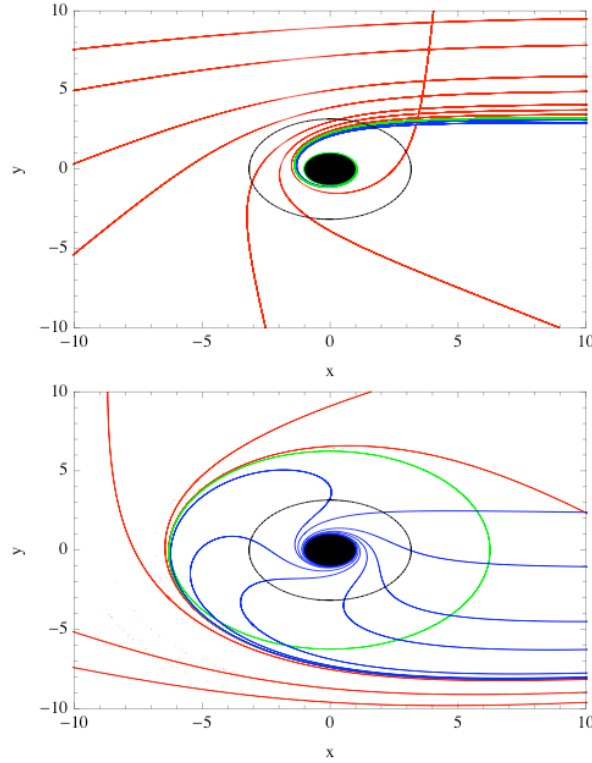


Figure 1: Rotating and counterrotating geodesics in the draining bathtub acoustic hole.

3. The basic equations for the scalar field perturbation ψ in the draining bathtub acoustic hole

Now we want to solve the Klein-Gordon equation (3) for the massless field ψ in the Lorentzian acoustic geometry, which in our case takes the form (4). We want to determine the modes of the field ψ . We can separate variables by the substitution

$$\psi(t, r, \phi) = R(r)e^{-i(\omega t - m\phi)}, \quad (9)$$

where $R(r)$ is a function of the coordinate r , ω is the frequency of the mode and m its azimuthal wave number. We now introduce a tortoise coordinate r_* defined by the condition $dr_*/dr = 1/(1 - A^2/c^2r^2)$. Explicitly, $r_* = r + \frac{A}{2c} \log \left| \frac{cr-A}{cr+A} \right|$, which in turn can be inverted to give $r(r_*)$. To obtain a Schrödinger-like equation we set $R(r) = Z(r)H(r)$ and find, first, Z as a function of (r, A, B, m) , $Z(r) = r^{1/2} f(r, A, B, m)$ which is not necessary to

give here explicitly. Then the Schrödinger-like equation for $H(r)$ is then

$$H_{,r_*r_*} + \left\{ \frac{1}{c^2} \left(\omega - \frac{Bm}{r^2} \right)^2 - \left(\frac{c^2 r^2 - A^2}{c^2 r^2} \right) \left[\frac{1}{r^2} \left(m^2 - \frac{1}{4} \right) + \frac{5A^2}{4r^4 c^2} \right] \right\} H = 0. \quad (10)$$

The wave equation (10) can be cast in a more useful form by performing the following rescalings, $\hat{r} = rA/c$, $\hat{\omega} = \omega A/c^2$, $\hat{B} = B/A$. We then get the Schrödinger-like equation

$$H_{,\hat{r}_*\hat{r}_*} + QH = 0, \quad (11)$$

with the generalized potential given by,

$$Q \equiv \left\{ \left(\hat{\omega} - \frac{\hat{B}m}{\hat{r}^2} \right)^2 - V \right\}, \quad V \equiv \left(\frac{\hat{r}^2 - 1}{\hat{r}^2} \right) \left[\frac{1}{\hat{r}^2} \left(m^2 - \frac{1}{4} \right) + \frac{5}{4\hat{r}^4} \right]. \quad (12)$$

The rescaling is equivalent to set $A = c = 1$ in the master wave equation, and at the same time the acoustic horizon obeys $\hat{r}_H = 1$. In addition, the horizon angular velocity is $\Omega = B/r_H^2$, i.e., $\Omega = \hat{B}$ in these units. Unless otherwise stated, we will omit hats in all quantities. The rescaled wave equation (11) will be the starting point of our analysis of QNMs [41, 42] (see also [43]). Then we study quasinormal modes [41, 42], power-law tails [41], superresonant phenomena [41], and sonic bombs [41] and plants.

4. Evolution of the perturbations in the draining bathtub acoustic hole: Quasinormal modes and tails

4.1 Generic features

The evolution of the perturbations of an acoustic hole has the same pattern as the evolution of perturbed black holes in spacetime. It can be divided into three parts: (i) Initially, there is the prompt response, which is dependent on the initial conditions. (ii) At an intermediate stage, the signal is predominantly an oscillating exponential which decays, giving rise to the quasinormal mode (QNM) oscillations, dependent on the black hole parameters alone, namely, mass, and angular momentum. (iii) At late times, the backscattering off the curvature creates a tail, a power law falloff of the field, which has a strong dependence on the asymptotic far region. Let us see in detail what really happens in the rotating draining bathtub acoustic hole.

4.2 Boundary conditions and asymptotic solutions

The QNMs of the rotating acoustic hole can be setup by defining appropriate boundary conditions and solving the corresponding eigenvalue problem,

m	$\omega_{QN}^{(1)}$	$\omega_{QN}^{(3)}$	$\omega_{QN}^{(6)}$
1	0.696-0.353i	0.321-0.389i	0.427-0.330i
2	1.105-0.349i	0.940-0.353i	0.945-0.344i
3	1.571-0.351i	1.465-0.353i	1.468-0.352i
4	2.054-0.352i	1.975-0.353i	1.976-0.353i

Table 1: The fundamental mode $n = 0$ of the rotating draining bathtub acoustic hole is shown for four different values of m . The first, third and sixth orders WKB approximation are displayed.

Eqs. (11)-(12). The boundary conditions are that close to the event horizon the solutions behave as $H \sim e^{-i(\omega-Bm)r_*}$, i.e., there are only ingoing waves. At spatial infinity the solutions of (11)-(12) behave as $H \sim e^{+i\omega r_*}$, i.e., there are only outgoing waves.

Then, for the wave equation (11)-(12) with the boundary conditions as given above, and assigned values of B and m (the rotational parameter and the angular index m , respectively) there is a discrete and infinite set of QN frequencies, ω_{QN} .

The QN frequencies are complex numbers. Since the time dependence is given by $e^{-i\omega t}$, the imaginary part describes the decay or growth of the perturbation. As it is expected the hole is stable against small perturbations, and thus ω_{QN} should have a negative imaginary part for an exponential time decay of the perturbation.

As it is usual, the QN frequencies ω_{QN} are ordered through the absolute value of their imaginary part, the modes being labeled by an integer n . The fundamental mode $n = 0$ will have the smallest imaginary part, in modulus.

4.3 Slowly decaying modes of non-rotating holes

The ringing behavior of a classical perturbation is controlled by the lowest QNMs. The overtones with higher frequency have a larger imaginary part, and so are damped faster and play no role. The fundamental mode with $n = 0$ is effectively responsible for the response of the acoustic hole to exterior perturbations.

The use of a WKB approximation with corrections up to the sixth order is certainly good enough. Such an approximation was developed in [6, 7], and to use it, Q in Eqs. (11)-(12) has to have a single maximum (see also [13]). For non-rotating holes, i.e., $B = 0$, this is true for $m \neq 0$. In Table 1 we present the fundamental mode $n = 0$, for different values of m in the WKB approximation in several orders. The real part of ω_{QN} scales nearly with m and the imaginary part is approximately constant as a function of m . In the large m limit one can show from the WKB formula [6] that ω_{QN}

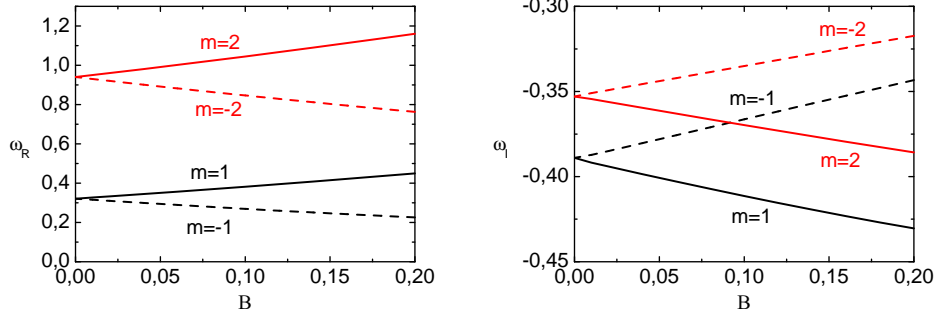


Figure 2: The real and imaginary frequencies of QNMs for the rotating draining bathtub acoustic hole. These frequencies, ω_R and ω_I respectively, are shown as a function of B (the rotating parameter) for different values of m (the perturbation azimuthal number).

behaves as

$$\omega \sim \frac{m}{2} - i \frac{2n+1}{2\sqrt{2}}, \quad m \rightarrow \infty, \quad (13)$$

and indeed already for $m = 4$ formula (13) yields excellent concordance with the results shown in Table 1.

To have some idea of the orders of magnitude involved, consider an $m = 2$ mode. Take typical values for a wave analogue experiment, such as those that can be directly inferred from [30], namely, $c = 0.31$ m/s, $r_H = 1$ m, $A = cr_H = 0.31$ m²/s, and obtain for the fundamental $n = 0$ QNM with $m = 2$, a frequency $\omega_R = 0.945 \times c^2/A = 0.293$ Hz and a damping timescale $\tau = 1/|\omega_I| = 1/0.344 \times A/c^2 = 9.37$ s.

For the case $m = 0$ the situation is more complicated, the WKB approximation is not usable because Q has more than one maxima. Using other sophisticated methods one can show that there are no $m = 0$ QNMs [43].

4.4 Slowly decaying modes of rotating holes

For rotating holes, the generalized potential, Eq. (12), has more than one extremum, so one has to use the WKB approximation with some care. It is necessary to take the only root that gives the correct non-rotating limit as $B \rightarrow 0$. It is this solution the one that corresponds to the QNMs of the rotating hole.

The WKB results we present can be trusted for $B \lesssim 0.1$. In Figure 2 the QNM frequencies for the draining bathtub acoustic hole are showed. In the left plot the real part of the fundamental QN frequency ω_R as a function of the rotation parameter B , for selected values of m , is shown. In the right plot the same is done for the imaginary part ω_I . Note that ω_R and $|\omega_I|$ increase with rotation for $m > 0$, while ω_R and $|\omega_I|$ decrease with rotation

for $m < 0$. Figure 2 seems to point out that it is possible an instability sets in for large Bm . To settle this issue an analysis beyond the WKB approximation is required.

Such an analysis of the QNMs in the high rotation regime, where the WKB approximation breaks down, was performed in [42], using a continued fraction analysis and numerical techniques. This was supplemented in the thorough work presented in [43] using a variety of techniques. It was found, as expected, that there are no instabilities for large Bm .

An interesting point worth mentioning is that the change of the QN frequency with rotation, although not drastic, can be used to apply a fingerprint analysis of the acoustic hole parameters (see [23] for the black hole case). Once we measure at least two QNM frequencies we may infer the hole parameters A and B . Carrying out such experiments in the laboratory can shed some light on the applicability of similar ideas to test the no-hair theorem in the astrophysical context [24].

4.5 Highly damped modes

QNMs with a large imaginary part, i.e., with a very large overtone number n , have interest for black holes in general relativity and other alternative theories of gravitation. Hod [26] proposed that these modes could be related to black hole area quantization. An analytical calculation of highly damped QNMs was first carried out by Motl for the Schwarzschild black hole [9, 10]. This analytical results are in agreement with numerical data [11, 12] (see also [8]).

To start with, let us consider a non-rotating hole, $B = 0$. Afterward we add rotation. For $B = 0$ the wave equation reduces to

$$\frac{d^2 H}{dr_*^2} + [\omega^2 - V(r)] H = 0, \quad (14)$$

with

$$V(r) \equiv \left(1 - \frac{1}{r^2}\right) \left(\frac{m^2 - 1/4}{r^2} + \frac{5}{4r^4}\right). \quad (15)$$

Following [9, 10] these modes are determined from $V(r)$ near the singular point $r = 0$. Thus $V \sim -5/36r_*^2$ (since $V \sim -5/4r^6$ and $r_* \sim -r^3/3$). Write $V = (j^2 - 1)/4r_*^2$ as one should for a field of spin j [9, 10]. Then one finds that in our case $j = 2/3$. Thus the scalar field of the perturbation has spin of $2/3$. A weird spin. The result in [9, 10] carries over directly, namely,

$$e^{4\pi\omega} = -(1 + 2 \cos \pi j). \quad (16)$$

However, $j = 2/3$ and $\cos(2\pi/3) = -1/2$, so $(1 + 2 \cos \pi j) = 0$. If we add rotation to the hole, i.e., if $B \neq 0$, a similar analysis implies the same result, namely, there are no asymptotic QN frequencies for these acoustic holes.

This result is quite hard to grasp. It may denote either that the real part grows without limit, or that it does not converge to a finite value. Whatever is the correct conclusion, an application of Hod's conjecture to these acoustic holes looks hopeless. The reason for this can perhaps be understood. In the analogue case, the laws of black hole thermodynamics cannot be recreated. It was argued by Visser [37] that black hole thermodynamics is directly related to Einstein equations. Undoubtedly, a well-known defect of analogue models is the fact that they can replicate the kinematical attributes of general relativity, but not the dynamics disclosed by Einstein equations. To obtain Hod's results [26] one has to assume a thermodynamic relation between black hole area and entropy. The lack of any such link for analogue models could account for the nonexistent relation between the QNM spectrum and area quantization.

4.6 Power-law tails

After the exponential QNM decay characteristic of the ringdown phase, black hole perturbations decay with a power-law tail [14] (see also [22]) due to the backscattering off the background curvature. One expects the same phenomenon holds in acoustic holes. Thus, we have computed the late-time tails of wave propagation in the draining bathtub and found that the field falloff at very late times is of the form

$$\psi \sim t^{-(2m+1)}, \quad (17)$$

where m is the azimuthal angular number [41]. This time exponent is a feature of any $(2+1)$ -dimensional spacetime, and not only of an acoustic hole [22].

5. Superresonance in the draining bathtub acoustic hole

Superradiance is a general phenomenon in physics. Zel'dovich [16, 17] pointed out that a cylinder made of absorbing material and rotating around its axis with frequency Ω can amplify modes of scalar or electromagnetic radiation of frequency ω , provided the condition

$$\omega < m\Omega, \quad (18)$$

where m is the azimuthal wave number with respect to the axis of rotation, is satisfied. This inequality is easier to understand if we work with periods instead of frequencies. Putting $T = 2\pi/\omega$ for the period of the wave, and $P = 2\pi/\Omega$ for the period of the cylinder rotation, then the inequality turns into $mT > P$. This means that there is superradiance when the wave stands

in nearby a sufficient period mT that it has time to absorb some of the cylinder rotational energy. Zel'dovich realized that, accounting for quantum effects, the rotating object should emit spontaneously in this superradiant regime. He further suggested that a Kerr black hole whose angular velocity at the horizon is Ω will show both amplification and spontaneous emission when the condition (18) for superradiance is satisfied. This suggestion was put on firmer ground by a substantial body of work (e.g., [18–22]). Black hole superradiance is related to the presence of an ergosphere, allowing the extraction of rotational energy from the black hole itself, and it is the wave equivalent of the Penrose process for particles [15].

The possibility of finding rotational superradiance in analogues, i.e., superresonance, was considered by Schützhold and Unruh [30] and Basak and Majumdar [45, 46] who computed in the low frequency limit the reflection coefficients $\omega r_H/c \ll 1$. Here we study further the phenomenon of superresonance for the rotating draining bathtub metric [41].

Consider an incident plane wave of frequency ω , azimuthal wave number m , and unit amplitude at infinity coming in from infinity towards the acoustic hole. A portion of this wave will be reflected back by the medium to infinity, the reflection coefficient being some complex number $R_{\omega m}$. In terms of the wave equation (11)-(12), this implies the following boundary condition at infinity,

$$H \sim R_{\omega m} e^{i\omega r_*} + e^{-i\omega r_*}, \quad r \rightarrow \infty. \quad (19)$$

At the sonic horizon ($r \rightarrow 1$, $r_* \rightarrow -\infty$) the solution has the following behavior

$$H \sim T_{\omega m} e^{-i(\omega - mB)r_*}, \quad r \rightarrow 1. \quad (20)$$

where $T_{\omega m}$ is the transmission coefficient. It gives the percentage of the wave that has passed through the horizon into the hole. Note that the wave equation for this superresonance problem and for the QNM problem is the same. However, each problem has their own distinct boundary conditions.

The Wronskian of a solution of (11) is constant since the equation has no first derivative in the radial coordinate. So compute it at the sonic horizon and at infinity and equate the computations. From Eqs. (19) and (20) one finds the following condition,

$$1 - |R_{\omega m}|^2 = \left(1 - \frac{mB}{\omega}\right) |T_{\omega m}|^2, \quad (21)$$

which can be seen as an energy conservation equation. For $\omega < mB$ the reflection coefficient obeys $|R_{\omega m}|^2 > 1$, which means there is superresonance. Refined conditions at r_H and at infinity can be used to compute numerically $R_{\omega m}$ [41].

Results for the rotating draining bathtub metric are shown in Fig. 3. The plots on the left show the superresonant amplification $|R_{\omega 1}|^2$ for $m = 1$ for

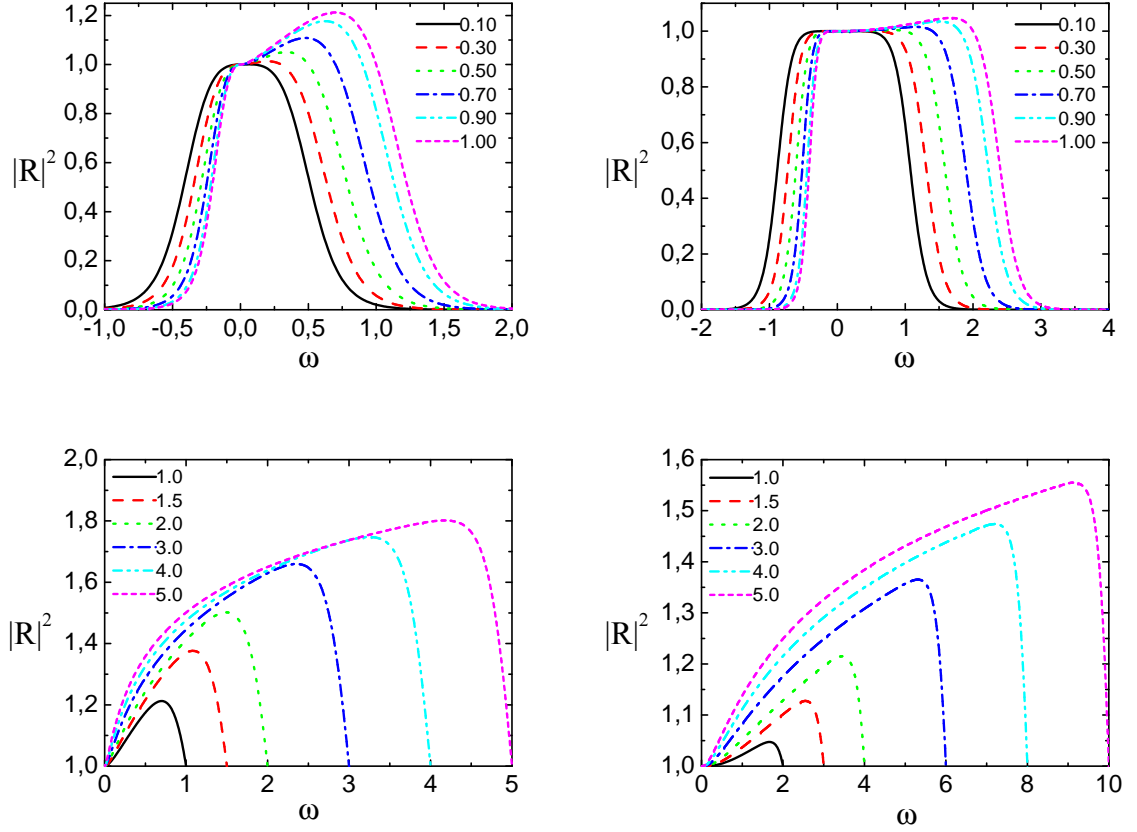


Figure 3: Plots for the superresonant amplification $|R_{\omega 1}|^2$ as a function of the wave frequency ω of the rotating draining bathtub acoustic hole. Top: Small rotation, $B \leq 1$, $|R_{\omega m}|^2$ as a function of ω for $m = 1$ (left plot) and $m = 2$ (right plot). Each curve corresponds to a different value of B . The reflection coefficient decays exponentially away from $\omega_{SR} = mB$ (the critical frequency for superresonance). For $B = 1$ the maximum amplification is 21.2% in the $m = 1$ case and 4.7% in the $m = 2$ case. Bottom: High rotation, $B > 1$, $|R_{\omega m}|^2$ as a function of ω for $m = 1$ (left plot) and $m = 2$ (right plot). Each curve corresponds to a different value of B . The plots show that for $B > 1$ superresonant amplification is very efficient.

some B s, while the plots on the right show the superresonant amplification $|R_{\omega 1}|^2$ for $m = 2$. The plots show that the reflection coefficient $|R_{\omega m}|^2 \geq 1$ in the superresonant regime, $0 < \omega < mB$, as it should. There are other interesting points. As B is increased the reflection coefficient also increases. For fixed B , there is a maximum for the reflection coefficient $|R_{\omega m}|^2$ at $\omega \sim mB$, decaying exponentially afterward as a function of ω outside the superresonant interval. This is the analogue of the superresonant amplification behavior for the Kerr metric [18]. In particular, zooming in one finds that, for $B = 1$ and $m = 1$ the maximum amplification is 21.2%, and for $B = 1$ and $m = 2$ the maximum amplification is 4.7%. See also the work of Oliveira, Dolan, and Crispino [43] for other developments.

6. The sonic bomb and plant: Superresonant instabilities in the rotating draining bathtub acoustic hole

6.1 Generic features

Kerr black holes are stable objects, but inside a mirror box they can build up an instability due to superradiance, originating a black hole bomb [21, 22] (see also [18]). Indeed, a detailed analysis performed by Cardoso, Dias, Lemos and Yoshida [22] for the Kerr black hole showed that the black hole bomb can be characterized by a set of complex resonant frequencies, the boxed quasinormal modes (BQNMs), which are responsible for the mode exponential growth and the bomb explosion.

The rotating draining bathtub acoustic hole also possesses an ergoregion which allows as well the possibility to make the system unstable. Suppose the system is enclosed in a reflecting mirror box with constant radius r_o . Now, throw into the hole a wave of frequency $\omega = \omega_R + i\omega_I$, such that $\omega_R < mB$. The wave is amplified by superresonant scattering, depleting the hole's rotational energy, and travels back to the mirror. There, it is reflected and moves again into the hole, now with increased amplitude. Through iterated reflections, the waves' amplitude grows exponentially with time. This is the analogue of the black hole bomb, it is the sonic bomb. Of course, the bomb can turn into a power plant if good use is made of the stored amplified energy.

One can argue in slightly more detail. The condition for the existence of standing waves in the region enclosed by the mirror is that the real part of a BQNM is proportional to $1/r_o$, i.e., $\omega_R \sim 1/r_o$, where r_o is the mirror radius. More precisely, defining λ as the wavelength of the standing wave, the condition is $\lambda \lesssim r_o$, or $\omega_R \gtrsim 1/r_o$, which in turn gives $r_o \gtrsim 1/\omega_R$. Now, the imaginary part of a BQNMs is proportional to $(\omega_R - mB)$, and so in order for the system to become unstable the system must be within

the superresonant condition, $\omega_R < mB$. Compounded with the standing wave condition this implies that the mirror should be located at a radius $r_o \gtrsim 1/mB$ in order for the system to become unstable. As time passes rotational energy is extracted from the system, the hole spins down and B decreases. For any given r_o the instability is eventually blocked, since the condition $r_o \gtrsim 1/mB$ is no longer obeyed.

6.2 Equation and boundary conditions

To solve the problem mathematically one has to solve once more the wave equation (11)-(12), but again with different boundary conditions. Assume that one is in the presence of a perfectly reflecting mirror, and impose two boundary conditions. At r_o one imposes a zero field, and at the horizon one demands the presence of purely ingoing waves, i.e.,

$$H(\omega_{BQN}, r_o) = 0, \quad H(r_H) \sim e^{-i(\omega_{BQN} - Bm)r_*}, \quad (22)$$

where ω_{BQN} are the complex BQNM frequencies. Then one can integrate the wave equation (11)-(12) outwards from the horizon. One can do it analytically and numerically.

6.3 Results

6.3.1 Analytical results

A matched asymptotic expansion is used to calculate analytically the unstable modes of the scalar field. One assumes $1/\omega \gg r_H$, i.e., the wavelength of the scalar field is much larger than the typical size of the acoustic hole. One considers the near region $r - r_H \ll 1/\omega$ and the far region $r - r_H \gg r_H$, and solves the radial equation for the two regions matching the solution in the overlapping region, $r_H \ll r - r_H \ll 1/\omega$.

In the near region the solution for H is some function with two terms, one term growing with r and the other decreasing with r . In addition, there is one constant of integration (one boundary condition has been used). In the far region the solution for H is a linear combination of Bessel functions with two constants, and again one term growing with r and the other decreasing with r . Matching the two solutions term by term gives a relation between the constants, in particular between the two constants of the far region solution as a function of the hole parameters and ω . Imposing further the box mirror condition for the far-field solution one gets another relation between the two constants of the far region solution as a function of the hole parameters, ω , and r_o . Thus a relation between ω and r_o (and the hole parameters) is obtained. The result for the rotating draining bathtub is

$$\omega_{BQN} = \omega_R + i\omega_I, \quad (23)$$

m	$j_{m,0}$	$j_{m,1}$	$j_{m,2}$
1	3.83171	7.01559	10.17347
2	5.13562	8.41724	11.61984
3	6.38016	9.76102	13.01520
4	7.58834	11.06471	14.37254
5	8.77148	12.33860	15.70017

Table 2: The first few values of the zeros of the Bessel function of integer order m , $j_{m,n}$, are given.

where

$$\omega_R = \frac{j_{m,n}}{r_o}, \quad (24)$$

$$\omega_I = -C (\omega_R - mB), \quad (25)$$

the $j_{m,n}$'s are zeros of the Bessel function of integer order m (see Table 2), with $n = 0$ being the fundamental mode, and $C = C(m, r_H, r_o)$ is some complicated function of no importance here. For a Kerr black hole bomb one gets $\omega_R = j_{l+1/2,n}/r_o$ [22], instead of (24).

Now, the scalar field ψ has time dependence $e^{-i\omega t}$, i.e.,

$$\psi \sim H e^{-i\omega_R t} e^{\omega_I t}. \quad (26)$$

Then $\omega_I > 0$ means, from Eq. (25), $\omega_R < mB$, the amplitude of the field grows exponentially and the BQNM becomes unstable with a growing time $\tau \sim 1/\omega_I$. On the other hand, $\omega_I < 0$ implies $\omega_R > mB$, and the amplitude decays.

Since $\omega_R = \frac{j_{m,n}}{r_o}$, the wave frequency is proportional to $1/r_o$. If the distance at which the mirror is located decreases, the allowed wave frequency increases, and there will thus be a critical r_o , r_{oc} say, at which the BQN frequency no longer satisfies the superresonant condition. Thus, with the superresonance condition $\omega_{BQN} < mB$, the instability switches off at

$$r_{oc} \simeq \frac{j_{m,n}}{mB}. \quad (27)$$

Since $j_{m,n}$ increases linearly with m (which is correct for high m 's, otherwise see Table 2 for low m 's) this means that the critical radius is practically m -independent. This is about what one can do analytically.

6.3.2 Numerical results

Numerically, one can perform calculations of the unstable modes of the scalar field by using, e.g, a Runge-Kutta method. The numerical results are

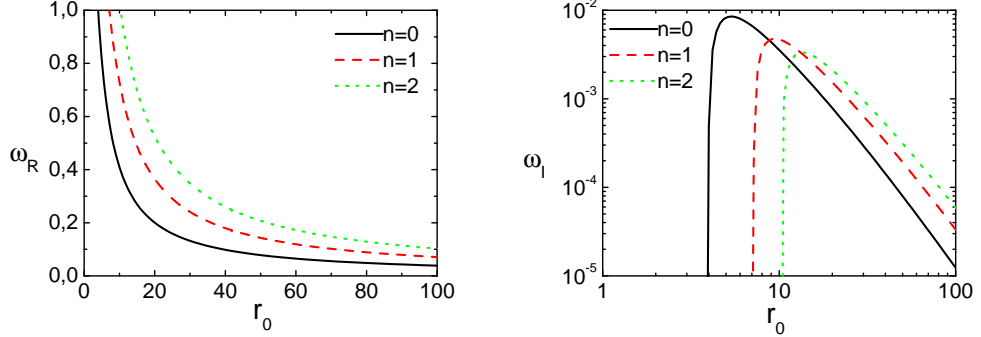


Figure 4: The frequencies of the BQNMs for $B = 1$ and $m = 1$ as a function of mirror location r_o for the rotating draining bathtub acoustic hole. The left plot shows the real frequencies and the right plot the imaginary ones. The three curves presented are for the fundamental mode $n = 0$, and the first and second overtones $n = 1, 2$, respectively. One sees that ω_R scales as $1/r_o$, as predicted analytically. The imaginary frequency ω_I crosses zero, and the instability abruptly evanesces at the critical radius r_{oc} .

in perfect concordance with the analytical predictions. In particular, this is true for small rotational parameters B . Note, however, that the real part of the BQN frequencies has a weak B -dependence. We picked $B = 1$, and $m = 1$, as an emblematic case, see Fig. 4. Note that when ω_I crosses zero the instability suddenly disappears. This happens at the critical radius r_{oc} , anticipated analytically. From the right plot of Fig. 4 we see that for any BQNM, the instability becomes more and more efficient as the mirror radius r_o becomes smaller, until eventually the mirror radius becomes small enough that the instability evanesces.

6.3.3 Remarks and orders of magnitude calculations

Some comments should be made:

(i) The real part of the BQN frequency grows, albeit slowly, with growing overtone number n . This means that higher overtones become stable at larger distances. In addition, they earn a smaller maximum growing rate.

(ii) With notable precision, the instability terminates when the critical radius is achieved, as concluded by the analytical formula complemented by the superresonance condition, that is: $r_{oc} \simeq \frac{j_{m,n}}{mB}$. We have also found from the analytical formula that since $j_{m,n}$ increases linearly with m this means that the critical radius is almost m -independent. This is attested numerically. However, at least when $B \lesssim 1$, the instability is not so proficient for high m as it is for small m . This is made clear in Fig. 5, where the ω_I , and thus the growth rates, of the $m = 1$ and $m = 2$ fundamental $n = 0$ modes for rotating acoustic holes are shown. As an example take $B = 0.3$.

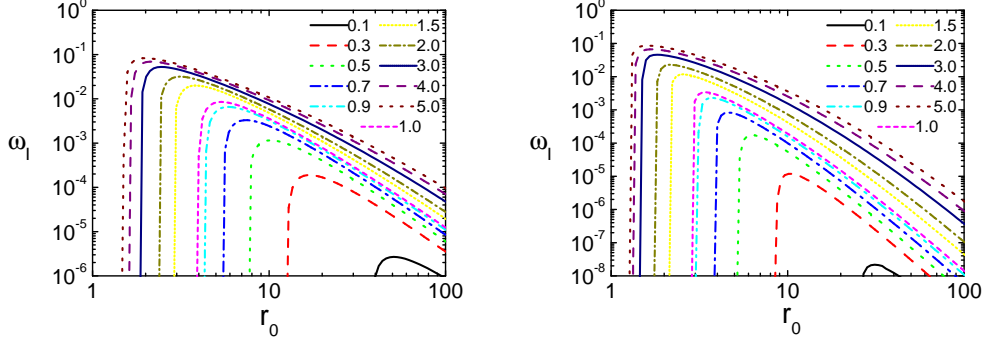


Figure 5: Imaginary frequencies ω_I of the fundamental mode $n = 0$ for BQNMs as a function of mirror location r_o for different values of the rotation parameter B of the rotating draining bathtub acoustic hole. The left plot is for $m = 1$, the right plot for $m = 2$. Note the difference of scale for the ω_I axis in each case. The imaginary frequency ω_I gives then the corresponding growth timescale.

Then the maximum growth rate for $m = 1$ is $\sim 10^{-4}$, and for $m = 2$ is $\sim 10^{-5}$. When $B > 1$, the growth rate for $m = 2$ becomes in effect of the same order as the growth rate for $m = 1$, as can be verified from the curves corresponding to $B = 5.0$.

(iii) One can find the response of the process by performing a straightforward calculation. When the instability arises the acoustic hole is releasing both energy and angular momentum, and the equation that connects these two quantities is $\Delta E \sim B \Delta J$. As B is decreased the critical radius r_{oc} increases. One now benefits from the mechanism itself by choosing a large B and an initial radius r_o for the mirror such that $r_o \simeq 2r_{o\max}$, where $r_{o\max}$ is defined as the radius of maximum growth timescale at the given B . As the hole expels angular momentum ΔJ , B is reduced. Given a mirror position r_o , the bomb finally shuts up when the condition $r_{oc} \simeq \frac{j_{m,n}}{mB}$ is obeyed. Measuring the difference in initial and final angular momentum ΔJ the extracted energy ΔE can be ascertained.

To have a hint of the orders of magnitude that can appear in this experiment, let us adopt $m = 1$ and an acoustic hole rotation parameter $\hat{B} = 1$, where we have recovered the hats, where hats distinguish dimensionless quantities from quantities with physical units. Let us then examine some characteristic parameters for the gravity wave analogue presented in [30]. So put, $r_H \sim 1$ m and $c \sim 0.31$ m s $^{-1}$. Then $B \sim 0.31$ m 2 s $^{-1}$. Once again, to full use the superresonance backscattering process the mirror should be positioned close to the maximum of ω_I , but not precisely at it. For instance, if the mirror is located at $\hat{r}_o \simeq 10 \sim 10$ m (cf. the right plot of Fig. 5), it is obtained $\hat{\omega}_I \simeq 4 \cdot 10^{-3}$ (in this case the maximum $\hat{\omega}_I$ would be $\hat{\omega}_I = 8.5 \cdot 10^{-3}$). This corresponds to a growth time $\tau \simeq 800$ s $\simeq 13$ minutes (at the maxi-

mum $\tau \simeq 6$ minutes is obtained). In rough terms, this indicates that the amplitude doubles every 13 minutes, and will be magnified by several orders of magnitude on timescales of a few hours. To shorten the characteristic timescale to seconds, one has to tune the horizon radius and wave velocity. For instance, working with $r_H \sim 0.1$ m and $c \sim 10$ m s⁻¹, a typical timescale of about 2 seconds is found. This seems an acceptable timescale to discern a sonic hole bomb in the lab.

(iv) As a final comment, we draw the attention to the fact that when we describe the acoustic hole surrounding by a reflecting mirror, we are thinking of a universal kind of mirror. In the shallow basin gravity wave analogue [30], the circular mirror reflects gravity water waves and is supposed to be a rubber band of radius r_o . A different option to realize a mirror could incorporate modifications in the sound waves dispersion relation, as would happen in the case of a change of the height of the basin [30]. Thus, given the right environment, one can build up an equipment that accumulates energy in the manner of amplified sound waves. This can be put to bad use as in a bomb, or to good use as in a sonic plant.

7. Conclusions

We have considered the $(2 + 1)$ -dimensional draining bathtub metric, a rotating acoustic hole metric, the analogue to the Kerr metric, and studied its QNMs, its superresonance features, its instabilities when surrounding it by a mirror and the possibility of turning it into a sonic bomb or a power plant. By adding a trivial third dimension, the setup can be transformed into a $(3 + 1)$ -dimensional draining bathtub. There are other metrics that describe acoustic holes. For instance there is the Schwarzschild analogue, a $(3 + 1)$ -dimensional spherically symmetric metric, called the canonical acoustic metric [29]. We have also studied the QNMs of this metric [41].

Acknowledgments

We thank Luis Carlos Crispino for the invitation and hospitality in the II Amazonian Symposium on Physics - Analogue Models of Gravity: 30 Years Celebration of the publication of Bill Unruh's paper "Experimental black-hole evaporation?", held in Universidade Federal do Pará, Belém, Brazil. This work was partially funded by Fundação para a Ciência e Tecnologia (FCT) - Portugal, through Projects PTDC/FIS/098962/2008 and PEst-OE/FIS/UI0099/2011.

Bibliography

- [1] C. W. Misner, K. S. Thorne, and J. A. Wheeler, *Gravitation* (Freeman, San Francisco, 1973).
- [2] B. Koch, M. Bleicher, and H. Stoecker, “Black holes at LHC?”, *Journal of Physics G* **34**, S535 (2007); arXiv:hep-ph/0702187.
- [3] J. P. S. Lemos, “Black holes: from galactic nuclei to elementary particles”, in *Proceedings of the XXIth Annual Meeting of the Brazilian Astronomical Society*, eds. F. Jablonski, F. Elizalde, L. Sodré Jr., V. Jablonski, (Instituto Astronômico e Geofísico–USP, S. Paulo, 1996), p. 57; arXiv:astro-ph/9612220.
- [4] C. V. Vishveshwara, “Scattering of gravitational radiation by a Schwarzschild black-hole”, *Nature* **227**, 936 (1970).
- [5] W. H. Press, “Long wave trains of gravitational waves from a vibrating black hole”, *Astrophysical Journal* **170**, L105 (1971).
- [6] B. F. Schutz and C. M. Will, “Black hole normal modes - A semianalytic approach”, *Astrophysical Journal* **291**, L33 (1985).
- [7] S. Iyer and C. M. Will, “Black-hole normal modes: A WKB approach. I. Foundations and application of a higher-order WKB analysis of potential-barrier scattering”, *Physical Review D* **35**, 3621 (1987).
- [8] H. P. Nollert, “Quasinormal modes of Schwarzschild black holes: The determination of quasinormal frequencies with very large imaginary parts”, *Physical Review D* **47**, 5253 (1993).
- [9] L. Motl, “An analytical computation of asymptotic Schwarzschild quasinormal frequencies”, *Advances in Theoretical and Mathematical Physics* **6**, 1135 (2003); arXiv:gr-qc/0212096.
- [10] L. Motl and A. Neitzke, “Asymptotic black hole quasinormal frequencies”, *Advances in Theoretical and Mathematical Physics* **7**, 307 (2003); arXiv:hep-th/0301173.

- [11] E. Berti and K. D. Kokkotas, “Asymptotic quasinormal modes of Reissner-Nordström and Kerr black holes”, *Physical Review D* **68**, 044027 (2003); arXiv:hep-th/0303029.
- [12] V. Cardoso, J. P. S. Lemos, and S. Yoshida, “Quasinormal modes of Schwarzschild black holes in four and higher dimensions”, *Physical Review D* **69**, 044004 (2004); arXiv:gr-qc/0309112.
- [13] R. A. Konoplya, “Quasinormal behavior of the D-dimensional Schwarzschild black hole and higher order WKB approach”, *Physical Review D* **68**, 024018 (2003); arXiv:gr-qc/0303052.
- [14] R. H. Price, “Nonspherical perturbations of relativistic gravitational collapse. I. Scalar and gravitational perturbations”, *Physical Review D* **5**, 2419 (1972).
- [15] R. Penrose, “Gravitational collapse: The role of general relativity”, *Rivista del Nuovo Cimento*, Numero Speciale **1**, 252 (1969).
- [16] Ya. B. Zel’dovich, “The generation of waves by a rotating body”, *Journal of Experimental and Theoretical Physics Letters JETP Letters* **14**, 180 (1971).
- [17] Ya. B. Zel’dovich, “Amplification of cylindrical electromagnetic waves reflected from a rotating body”, *Journal of Experimental and Theoretical Physics JETP* **35**, 1085 (1972).
- [18] S. A. Teukolsky and W. H. Press, “Perturbations of a rotating black hole. III - Interaction of the hole with gravitational and electromagnetic radiation”, *Astrophysical Journal* **193**, 443 (1974).
- [19] W. G. Unruh, “Second quantization in the Kerr metric”, *Physical Review D* **10**, 3194 (1974).
- [20] J. D. Bekenstein and M. Schiffer, “The many faces of superradiance”, *Physical Review D* **58**, 064014 (1998).
- [21] W. H. Press and S. A. Teukolsky, “Floating orbits, superradiant scattering and the black-hole bomb”, *Nature* **238**, 211 (1972).
- [22] V. Cardoso, O. J. C. Dias, J. P. S. Lemos, and S. Yoshida, “Black-hole bomb and superradiant instabilities”, *Physical Review D* **70**, 044039 (2004); arXiv:hep-th/0404096.
- [23] F. Echeverria, “Gravitational-wave measurements of the mass and angular momentum of a black hole”, *Physical Review D* **40**, 3194 (1989).

- [24] C. M. Will, “Testing the general relativistic no-hair theorems using the galactic center black hole SgrA*”, *Astrophysical Journal Letters* **674**, L25 (2008); arXiv:0711.1677 [astro-ph].
- [25] S. W. Hawking, “Particle creation by black holes”, *Communications in Mathematical Physics* **43**, 199 (1975).
- [26] S. Hod, “Bohr’s correspondence principle and the area spectrum of quantum black holes”, *Physical Review Letters* **81**, 4293 (1998); arXiv:gr-qc/9812002.
- [27] J. P. S. Lemos, “Black holes and fundamental physics”, in the *Proceedings of the Fifth International Workshop on New Worlds in Astroparticle Physics*, eds. Ana M. Mourão et al. (World Scientific, Singapore, 2006), p. 71; arXiv:gr-qc/0507101.
- [28] W. G. Unruh, “Experimental black-hole evaporation?”, *Physical Review Letters* **46**, 1351 (1981).
- [29] M. Visser, “Acoustic black holes: horizons, ergospheres, and Hawking radiation”, *Classical and Quantum Gravity* **15**, 1767 (1998); arXiv:gr-qc/9712010.
- [30] R. Schützhold and W. G. Unruh, “Gravity wave analogs of black holes”, *Physical Review D* **66**, 044019 (2002); arXiv:gr-qc/0205099.
- [31] M. Visser and S. Weinfurtner, “Vortex geometry for the equatorial slice of the Kerr black hole”, *Classical and Quantum Gravity* **22**, 2493 (2005); arXiv:gr-qc/0409014.
- [32] C. Barceló, S. Liberati, and M. Visser, “Analogue gravity”, *Living Reviews in Relativity* **8**, 12 (2005); arXiv:gr-qc/0505065.
- [33] B. Reznik, “Origin of the thermal radiation in a solid-state analogue of a black hole”, *Physical Review D* **62**, 044044 (2000); arXiv:gr-qc/9703076.
- [34] L. J. Garay, J. R. Anglin, J. I. Cirac, and P. Zoller, “Sonic black holes in dilute Bose-Einstein condensates”, *Physical Review A* **63**, 023611 (2001); arXiv:gr-qc/0005131.
- [35] C. Barceló, S. Liberati, and Matt Visser, “Refringence, field theory, and normal modes”, *Classical and Quantum Gravity* **19**, 2961 (2002); arXiv:gr-qc/0111059.
- [36] W. G. Unruh, “Sonic analogue of black holes and the effects of high frequencies on black hole evaporation”, *Physical Review D* **51**, 2827 (1995); arXiv:gr-qc/9409008.

- [37] M. Visser, “Hawking radiation without black hole entropy”, *Physical Review Letters* **80**, 3436 (1998); arXiv:gr-qc/9712016.
- [38] U. R. Fischer and G. E. Volovik, “Thermal quasi-equilibrium states across Landau horizons in the effective gravity of superfluids”, *International Journal of Modern Physics D* **10**, 57 (2001); arXiv:gr-qc/0003017.
- [39] S. Weinfurtner, E. W. Tedford, M. C. J. Penrice, W. G. Unruh, and G. A. Lawrence, “Measurement of stimulated Hawking emission in an analogue system”, *Physical Review Letters* **106** 021302 (2011); arXiv:1008.1911 [gr-qc].
- [40] C. Barceló, S. Liberati, S. Sonego, and M. Visser, “Causal structure of acoustic spacetimes”, *New Journal of Physics* **6**, 186 (2004); arXiv:gr-qc/0408022.
- [41] E. Berti, V. Cardoso, and J. P. S. Lemos, “Quasinormal modes and classical wave propagation in analogue black holes”, *Physical Review D* **70**, 124006 (2004); arXiv:gr-qc/0408099.
- [42] V. Cardoso, J. P. S. Lemos, and Shijun Yoshida, “Quasinormal modes and stability of the rotating acoustic black hole: numerical analysis”, *Physical Review D* **70**, 124032 (2004); arXiv:gr-qc/0410107.
- [43] S. Dolan, L. A. Oliveira, and L. C. B. Crispino, “Resonances of a rotating black hole analogue”, *Physical Review D* **85**, 044031 (2012); arXiv:1105.1795 [gr-qc].
- [44] M. E. M. Marques, “Acoustic black holes and superresonance mechanisms”, M.Sc. Thesis, Physics Department, Instituto Superior Técnico, (Lisbon, 2011).
- [45] S. Basak and P. Majumdar, “Superresonance from a rotating acoustic black hole”, *Classical and Quantum Gravity* **20**, 3907 (2003); arXiv:gr-qc/0203059.
- [46] S. Basak and P. Majumdar, “Reflection coefficient for superresonant scattering”, *Classical and Quantum Gravity* **20**, 2929 (2003); gr-qc/0303012 .